Iron-modified Biochar Derived from Rice Straw for Aqueous Phosphate Removal

Usarat Thawornchaisit*, Korawan Donnok, Natchaphat Samphoanoi, Pimwimon Pholsil

Department of Chemistry, Faculty of Science
King Mongkut's Institute of Technology Ladkrabang, Bangkok, Thailand

Received: 17 May 2019, Revised: 19 July 2019, Accepted: 7 August 2019

Abstract

Conversion of rice straw to biochar, followed by chemical modification of the biochar with iron salts under alkaline conditions can turn agricultural biomass waste into a useful adsorbent material for phosphorus removal. Study of the rice straw-to-biochar conversion process at various pyrolysis temperatures showed that biochar yield decreased with increased pyrolysis temperature: The yield of stable organic matter and specific surface area was found to be optimum at 400°C. An Fe coating process, through direct precipitation of $FeCl_3.6H_2O$ or co-precipitation of $FeCl_3.6H_2O$ and $FeSO_4.7H_2O$ on biochar, led to Fe-modified rice straw biochars. Based on physical appearance, SEM, FT-IR and XRF, we confirmed that Fe was well retained in the biochar. The pH_{pzc} was approximately 7.6 and 8.0 for Fe(III)+Fe(II)-modified biochar and Fe(III) modified biochar. Therefore, the modified biochar could attract negatively charged phosphate species in a system, like natural water or domestic wastewater, where pH is normally less than their pH_{pzc}. In laboratory batch adsorption tests, phosphate removal efficiency was enhanced, rising from about 35.4% in the unmodified biochar to 69.5% in Fe(III)+Fe(II)-modified biochar and 83.0% in Fe(III) modified biochar.

Keywords: biochar modification, phosphorus removal, pyrolysis
DOI 10.14456/cast.2019.22

1. Introduction

Phosphorus is an essential nutrient, which is vital for the growth of aquatic plants. However, phosphorus becomes a pollutant, when it is present in excessive amounts in aquatic environments. Excess phosphorus from runoff into water bodies, such as lakes, creeks and rivers, can cause eutrophication an environmental problem caused by excessive growth of algae and other aquatic plants. This phenomenon often leads to deterioration in the aquatic ecosystem quality, for example, development of anoxic conditions and decreased biodiversity [1, 2]. Discharge of municipal wastewaters is one of the main causes of eutrophication, since the wastewaters are rich in

*Corresponding author: E-mail: usarat.th@kmitl.ac.th

phosphorus [1]. Therefore, wastewater treatment is important in order to reduce phosphorus levels from the effluent, limit phosphorus load in receiving water bodies, and subsequently protect public health.

Phosphorus in water occurs in both dissolved and particulate forms. However, most of the phosphorus discharged by wastewater treatment facility plants (WWTPs) is in the dissolved form and is mainly orthophosphate [3]. Previously, phosphorus removal, rather than recovery, emerged with the primary attention given to lowering phosphorus levels in effluents for safe discharge into surface waters [4], which, in turn, would inhibit undesirable algal growth in sensitive surface waters [3, 5]. Thus, technologies for phosphorus pollution control tended to be more focused and oriented towards phosphorus removal, whereas technologies that focus on recovery have received less attention [4]. In 2015, a report on "World Fertilizer Trend and Outlook to 2018", published by the United Nations Food and Agriculture Organization, showed an increasing world phosphate fertilizer demand between 2014 and 2018, with 58 % of the increase expected to be in Asia. Today, the primary source of phosphorus in fertilizers is natural minerals, for example, mined phosphate rock [4]. Unfortunately, phosphate rock is a finite, nonrenewable resource [4] and is listed as one of the critical raw materials for the European Union in their 2017 final report - "Study on the review of the list of critical raw materials: Criticality Assessment" [6]. The growing concern about phosphorus future availability and its detrimental environmental impact have driven phosphorus recovery to become crucial. Thus, research on the treatment of phosphorus-containing wastewater is currently focused more on development of technology that can recover phosphorus from the secondary source (like domestic and industrial wastewater) and reuse the recovered P products for agricultural and industrial purposes [7].

Biochar, the carbon-rich residues from pyrolysis or incomplete combustion of biomass, has increasingly been recognized as an efficient and cost-effective sorbent for removal of aqueous organic and inorganic contaminants, such as textile dyes, phenolics, pesticides, polycyclic aromatic hydrocarbons, heavy metals, and metalloids [8-10]. For example, straw derived biochar can effectively remove malachite green, which resists aerobic digestion, due to its reported toxic effects [11]. With acid pretreatment, straw-based biochar was also used as a substitute for activated carbon to remove reactive brilliant blue and rhodamine B [12]. Biochar was recognized as an effective sorbent for heavy metals especially the cationic forms due to the presence of oxygen-containing carboxyl, hydroxyl, and phenolic surface functional groups and high-porous structure [10, 13]. As the surfaces of biochar is predominantly negatively charged, the sorption of anionic forms of pollutants such as arsenates, nitrates or phosphates is relatively low [14, 15]. Therefore, a modification of the biochar structure and surface properties is needed to enhance the affinity for anionic contaminants and, consequently, its environmental benefits [14, 16]. Significantly, the study of the use of biochar to remove phosphates from water has been limited, compared to the study of remediation of other common water pollutants [17], thus we need to fill in the information gap in the research on practical applications of biochar and well-engineered biochar that has been modified for phosphate removal from water.

Rice straw (*Oryza sativa*), left over from rice harvesting, is one of the most abundant lignocellulosic waste materials world-wide [11]. From 0.7 to 1.4 kg of rice straw is produced for each kilogram of milled rice, depending on variety, stubble cutting-height and moisture content during harvest [18]. FAO estimated that about 770 million tonnes of rice was produced in 2018 [19]. Thus, rice straw became available in similar quantities and, consequently, methods for rice straw use and disposal are needed. In Thailand, rice straw was one of the top three unused lignocellulosic agricultural by-products in 2013 [20]. Direct open burning in fields is a common option for disposal, but this causes serious air pollution. Farmers often offer rice straw as a feed for ruminants, but untreated rice straw is not an ideal feed due to the low nutritive value of the highly lignified materials. Hence, effective rice straw consumption strategies that are economically feasible are badly needed. Here, we show that rice straw can produce biochar that is able to adsorb phosphate

from aqueous solutions. This adds value to this agricultural by-product and provides a potential adsorbent for nutrient removal. Further, the spent adsorbent is nutrient-enriched biochar, which can subsequently be applied as fertilizer. We selected an iron modified method to improve the phosphate adsorption, since the method is simpler and more efficient than other treatments such as activation by sulfuric acid and lanthanum [21]. In conclusion, we confirmed the feasibility of using rice straw-derived biochar for aqueous phosphate removal and showed that phosphorus removal capacity can be enhanced by adding iron as the char is produced.

2. Materials and Methods

2.1 Preparation of adsorbent

2.1.1 Biochar production with different pyrolysis temperatures

Rice straw was obtained from a paddy field in Chachoengsao Province (13.69028N, 101.07028E). Prior to pyrolysis, the rice straw was chopped into ~20-30 mm lengths and ground to pass through a 70-mesh (210 μm) sieve. The straw was oven dried at 103-105ºC until it reached constant weight. The dried straw was put into a 100 ml ceramic crucible, covered with a lid, and pyrolyzed under limited oxygen conditions in a muffle furnace (Thermolyne Furnace 6000) at 300, 400, 500 and 600ºC for 4 h. Once cooled to room temperature, the biochar was stored in sealed sample bags.

2.1.2 Synthesis of Fe-modified biochar

The selected biochar was modified with iron following the method described by Yang *et al.* [21]. Fe(III)-modified biochar was prepared by adding 1 g biochar into 30 ml aqueous solution containing 2.18g $FeCl_3.6H_2O$. The suspension of biochar and Fe solution was stirred vigorously at 150 rpm for 30 min, and this was followed by a dropwise addition of 1 M NaOH solution until the pH reached ~11. The suspension was continuously stirred for 45 min and aged overnight without further stirring. The separated modified biochar samples were washed several times with deionized water and dried at 105ºC until they reached constant weight. The preparation of biochar doped with co-precipitation of Fe^{2+}/Fe^{3+} was similar, except that the solution contained 1.17 g $FeSO_4.7H_2O$ and 1.09 g $FeCl_3.6H_2O$.

2.2 Characterization of biochar

For unmodified or virgin rice straw-derived biochar, yield (%) was determined by comparing the weight of the biochar to the weight on a dry basis of the ground rice straw used for pyrolysis. Oxidizable organic carbon content (OC) was determined by the wet oxidation method with potassium dichromate [22]. Loss on Ignition (LOI), Stable Organic Matter (SOM) and Stable Organic Matter Yield Index (SOMYI) were determined and calculated following the methods of Halshejani *et al.* [23]. Specific surface area (SSA) was measured by methylene blue adsorption and calculated following Kaewprasit *et al.* [24]. For unmodified and Fe-modified biochars, the morphological properties of the biochars were determined by scanning electron microscopy (SEM, JEOL, JSM-6355FE). The functional groups on the biochar surface were determined from a Fourier transform infrared spectrum (FTIR, Shimadzu, IRTracer-100) in the 400-4000 cm^{-1} range. The iron contents of modified biochars was examined using X-ray Fluorescence Spectrometry (XRF, Bruker Optic, SRS3400). The pH at point of zero point charge (pH_{pzc}) of the Fe-modified biochars was measured by adjusting the pH of 50 mL 0.01 mol/l NaCl solution to a value between 3 and 11, and

noting the initital pH value (pH_i). Then, 0.15 g of the Fe-modified biochars was added to a conical flask and the flask was shaken in an incubator shaker at 120 rpm for 24 hours. The final pH (pH_f) of the solutions separated by centrifugation was measured, and the pH_{pzc} was found at the point where pH_f - pH_i = 0 from a plot of ΔpH vs pH_i.

2.3 Phosphate removal tests

The phosphorus removal capacity of rice straw-derived biochar and Fe-modified biochars was measured by mixing various amounts of the biochars with 50 mL of 2.5 mg P l^{-1} solution in 125 mL Erlenmeyer flasks at room-temperature. The flasks were then shaken in a mechanical shaker at a constant speed of 150 rpm. At selected time intervals, the flasks were withdrawn and the suspensions were immediately filtered through a 0.45 μm filter. The concentration of remaining phosphorus in the filtrate was determined by the ascorbic acid method [25]. The phosphate removal from aqueous solution (%R) was calculated from:

$$\%R = \frac{(C_o - C_e)}{C_o} \times 100 \quad (1)$$

where C_0 (mg/l) was the initial and C_e (mg/l) was the residual concentration of phosphorus in solution.

3. Results and Discussion

3.1 Rice straw-derived biochar physicochemical properties

Previous research indicated that pyrolysis temperature significantly influences the carbon content of biochar and its surface properties (pore structure, surface area, and capability), which in turn play an important role in the physical or chemical attachment of mineral ions to the biochar structures. Therefore, a pyrolysis temperature that provided a high surface area and yielded stable organic matter (SOM) content of the biochar was determined first. The properties of the biochars produced at different pyrolysis temperatures are shown in Table 1.

From Table 1, the biochar yield decreased with an increase in temperature during slow pyrolysis. Similar trends were also observed by Jiang *et al.* [26] and Wang *et al.* [27], where a decrease in biochar yield was observed with increased pyrolysis temperature between 200ºC and 700ºC. The observed behavior is due to the increase in the rate of dehydration and, in particular, a significant loss of volatile organic matter at higher pyrolysis temperatures, as shown by the decrease of loss on ignition (LOI) of the biochar. In addition, the higher the temperature during pyrolysis is, the lower the oxidizable organic carbon (OC) of the biochar is. This reflects an increase in ash content in the biochar at high pyrolysis temperatures, which is consistent with the findings of Halshejani *et al.* [23] and Masto *et al.* [28]. Since the biochar will be exposed to either physical or chemical processes during iron modification, in order to enhance its adsorption capacity for contaminant removal from water and wastewater, the stability of the biochar is critical [16, 29]. The stable organic matter contents (SOM) and the stable organic matter yield index (SOMYI) reflect this characteristic as the importance of both characteristics to the biochar adsorption capacity was stated by Halshejani *et al.* [23] and Masto *et al.* [28]. The SOM of the biochar increased with temperature up to 400ºC, but further increase in temperature yielded lower SOM in the biochar (Table 1). The SOMYI also showed a similar pattern suggesting that biochar produced at 400ºC should be selected for further study. In addition, pyrolysis temperature affected the biochar surface

area, which increased from 66.4 m^2/g to 75.9 m^2/g when pyrolysis temperature was increased from 300°C to 400°C. Maximum specific surface area of rice straw-derived biochar, determined by methylene blue adsorption [24], occurred at 400°C (Table 1). Increase in pyrolysis temperature can cause pore blocking substances to be driven out or thermally cracked, leading to a significant increase in the externally accessible surface area [30]. However, the specific surface area decreased at temperatures above 400°C (Table 1). Previous studies have also reported this and it is attributed to structural ordering and micropore coalescence, resulting in a thermal deactivation of the biochar [31-33]. Since maximum SOMYI and SSA occurred at 400°C, biochar produced at this temperature (BC400) was selected for different levels of iron modification.

Table 1. Properties of rice straw-derived biochar at different pyrolysis temperatures

	Pyrolysis temperature (°C)			
Parameter	**300**	**400**	**500**	**600**
Yield (%)	27.0	22.7	18.6	14.8
Loss on Ignition (LOI, %)	64.6	58.4	47.2	33.6
Oxidizable organic carbon (%)	36.8	19.6	18.0	12.4
Stable Organic Matters (SOM, %)	1.20	24.6	16.2	12.2
Stable Organic Matter Yield Index (SOMYI)	0.3	5.6	3.0	1.8
Specific surface area (m^2/g)[a]	66.4	75.9	48.6	14.9

[a]Calculation method followed Kaewprasit *et al.*[24]

3.2 Fe-modified biochar physicochemical properties

3.2.1 Physical appearance

The ground rice straw samples had a golden brown color (Figure 1a). After pyrolyzing at 400°C for 4 hours, the samples were converted to the blackened biochar (Figure 1b). Small amounts of gray dust were also observed in the biochar, suggesting the presence of some ash. Fe-modified biochars had colors in the red to dark brown range (Figure 1c and 1d), which differed from the biochar without added Fe. The color confirmed that iron was well loaded into the biochar.

Figure 1. Appearance of original input (a) and biochars after pyrolysis (b-d)

3.2.2 Surface structure by SEM

Figure 2 shows SEM images of iron modified biochars compared to the unmodified biochar. The surface of the virgin biochar was smooth, while the surfaces of Fe(III)-modified biochar and Fe(III)+Fe(II) modified biochar were rough, cracked into fragments and had some small particles on their surface.

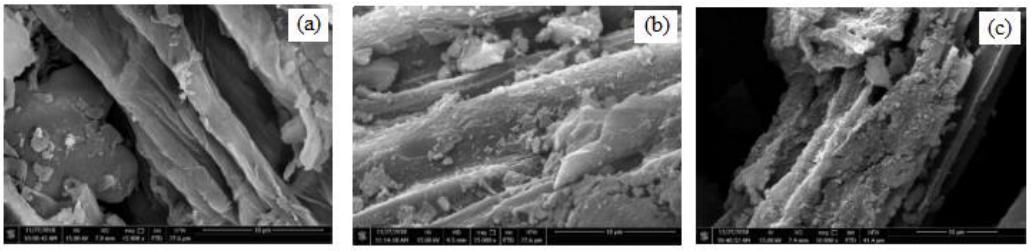

Figure 2. Scanning Electron Micrographs (SEM) of (a) BC400, (b) Fe(III)-modified biochar and (c) Fe(III)+Fe(II)-modified biochar

3.2.3 Functional groups by FT-IR

The FT-IR spectra of the biochar prepared from pyrolyzing rice straw at 400°C and the Fe-modified biochars were captured to determine the various functional groups in the biochars. The presence of several peaks common to all biochars was observed in the spectra of all three samples (Figure 3). The broad peak at ~3420 cm^{-1} and the peak near 1384 cm^{-1} were attributed to -OH stretching vibrations [21, 34]. The peak at ~2920 cm^{-1} corresponded to the aliphatic C-H stretching vibration, while peaks at ~1615 cm^{-1} were assigned to C = O or C = C stretching in aromatic groups [35]. The wide peak at 3420 cm^{-1} in both types of Fe-modified biochars compared with the unmodified biochar is attributed to the use of $FeCl_3$ in the co-precipitation stage, which led to the partial coating of the biochar surface with ferric oxyhydroxide (FeOOH) - also observed by Kulaksiz *et al.* [36]. The intense band at ~1100 cm^{-1} in the unmodified biochar (Figure 3a), which is attributed to C-O vibration [34], was shifted to ~1000 cm^{-1} in the Fe-modified biochars, suggesting that chemical interaction occurred on the modified biochar surface. Yang *et al.* [21] suggested that the band at 1067 cm^{-1} represented Fe-OH, indicating the immobilization of iron on the biochar.

3.2.4 Elemental composition by XRF

XRF analyses were carried out to determine the elemental composition of biochars before and after Fe modification, with results shown in Table 2. The concentration of some minerals, including Si, Ca, Mg and Mn, decreased in the Fe modified biochars compared to those found in unmodified biochar (BC400). These observations were attributed to the dissolution of these minerals under alkaline conditions [37], which could have had a significant impact on the textural properties of biochar, and subsequently on the success on biochar modification process. This assumption was further confirmed by the observed increase in concentration of Fe_2O_3 in both Fe(III)+Fe(II) modified biochar and Fe(III) modified biochar.

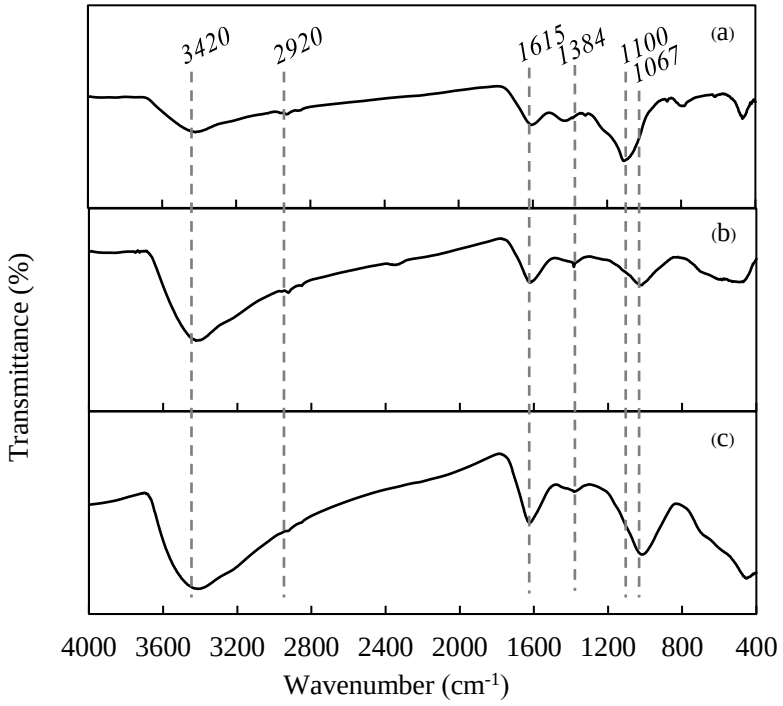

Figure 3. FTIR spectra of (a) BC400, (b) Fe(III) modified biochar and (c) Fe(III)+Fe(II) modified biochar

Table 2. XRF analysis of biochar and Fe-modified biochars

Formula	**BC400**	**Modified biochar**	
		Fe(III)	**Fe(III)/Fe(II)**
CaO	6.58	3.55	3.07
CuO	0.29	0.30	0.28
Cl	11.2	0.53	0.42
Fe_2O_3	0.79	73.0	66.9
K_2O	20.2	n.d.	n.d.
MgO	4.91	1.94	1.98
MnO	0.37	n.d.	n.d.
Na_2O	1.37	1.63	2.22
P_2O_5	2.15	0.43	0.82
SiO_2	49.2	17.0	22.6
SO_3	5.31	0.54	1.11

3.2.5 Point of zero charge (pH_{pzc})

The pH_{pzc} of Fe modified biochars was determined in order to demonstrate the tolerance of the adsorbent towards variation in solution pH [35]. From Figure 4, the pH_{pzc} of Fe(III) modified biochar was approximately 8.0, while the pH_{pzc} of Fe(III)+Fe(II) modified biochar was about 7.6, implying that the Fe-modified biochars would be positively charged when they were applied to treat phosphates in natural water or domestic wastewater (where $pH<pH_{pzc}$), and could effectively remove and recover phosphate owing to the strong electrostatic attraction.

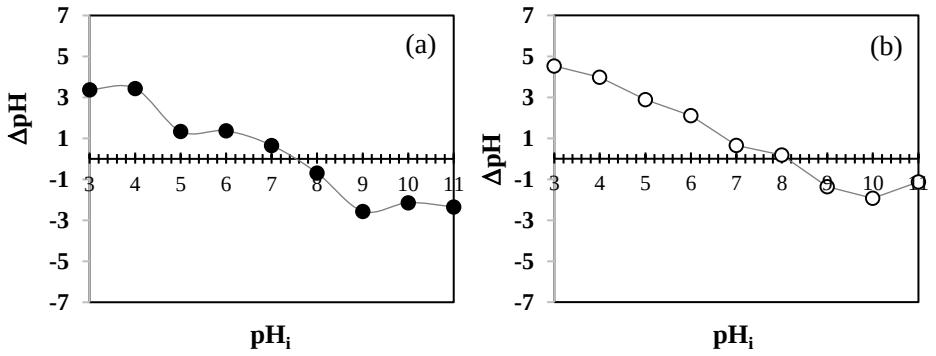

Figure 4. Plots of ΔpH versus initial pH for determination of pH_{pzc} of (a) Fe(III)+Fe(II) modified biochar, and (b) Fe(III) modified biochar

3.3 Phosphate removal

3.3.1 Effect of contact time

Figure 5 shows the phosphorus removal efficiency of unmodified biochar (BC400) and the Fe-modified biochars. It can be seen that phosphate removal efficiency of Fe-modified biochars was higher than BC400. In a 1 h contact time, Fe(III)-modified biochar and Fe(III)+Fe(II)-modified biochar removed more than 50% of phosphorus, suggesting that the adsorption capacity of Fe-modified biochars, for removing phosphate, was rapid in the beginning stages of contact. An increase in phosphorus removal occurred in both types of modified biochar as contact time was extended to 24 h. Phosphate removal efficiencies after 24 hours contact time were 70% for Fe(III)+Fe(II)-modified and 83% for Fe(III)-modified biochar. In the same time, the unmodified biochar (BC400) removed only ~35% of phosphorus. Previous studies reported that the biochar produced from sesame straw exhibits positive phosphate adsorption when pyrolysed at 500 and 700°C [38]. This phenomenon was attributed to the presence of Ca and Mg in the biochar, which chemically react with phosphate through two main mechanisms: precipitation of P through chemical reaction with these metal ions, and surface deposition of P on Mg crystals on biochar surfaces [38-39]. Compared to unmodified biochar, improved phosphate removal efficiency in Fe-modified biochars was attributed to two factors in the iron modification; it changed the surface and the porous structure of the biochar and thus provided more attractive sites for phosphate adsorption [21].

The valence state of iron in the biochars also played important role in phosphate removal. Biochar with Fe^{3+} in alkaline conditions showed higher phosphate removal efficiency than biochar with co-precipitation of Fe^{3+}/Fe^{2+} (Figure 5). The presence of $Fe(OH)_3$ and Fe_2O_3 which should be more prevalent in the Fe(III)-modified biochar compared to Fe(III)+Fe(II) modified biochar

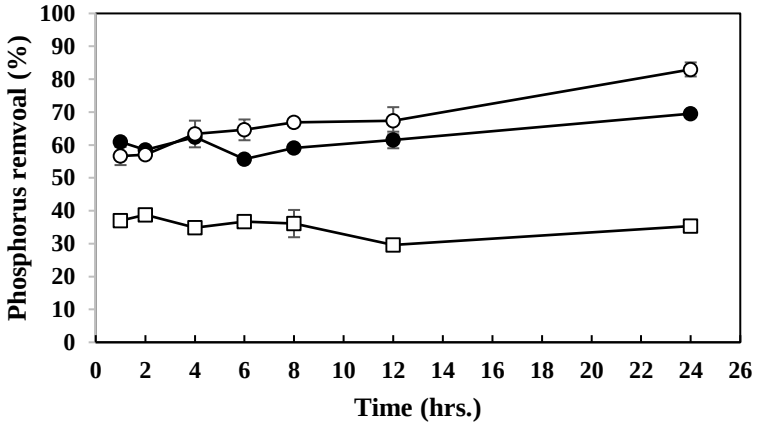

Figure 5. Phosphate removal capacity of (□) BC400, (O) Fe(III) modified biochar and (●) Fe(III)+Fe(II) modified biochar (pH: 7; adsorbent dose: 2g/L; PO_4^{3-}-P: 2.5 mg/l).

explains why the Fe(III) removed phosphate better. Fe(III)'s higher valence state led to a greater affinity for a hard base like PO_4^{3-}, thus reaction between PO_4^{3-} and Fe^{3+} would be more favorable through a combination of electrostatic attraction, surface complexation and anion exchange as reported by Yang *et al.* [21]. The amount of iron in the biochar also played an important role in phosphate removal. XRF analysis (see Table 2) revealed that Fe(III)-modified biochar contained higher iron concentration than Fe(III)+Fe(II)-modified biochar, thus it removed phosphate more efficiently.

3.3.2 Effect of biochar dosage

Adsorbent dosage in water influenced phosphate removal of biochars, especially the Fe-modified biochars (Figure 6). With an increase in dose of Fe(III)-modified biochar from 2 to 16 g/l, phosphate removal efficiency increased to 90%. A similar trend was observed when Fe(III)+Fe(II)-modified biochar was used to treat phosphates in water (Figure 6). This was due to the availability of active sites and increase in surface area at higher dose [23]. On the other hand, increase in dose had no significant effect on phosphate removal in the case of the original biochar, BC400. This further confirmed that iron treatment of these biochars changed the biochar surface properties, resulting in better phosphate removal.

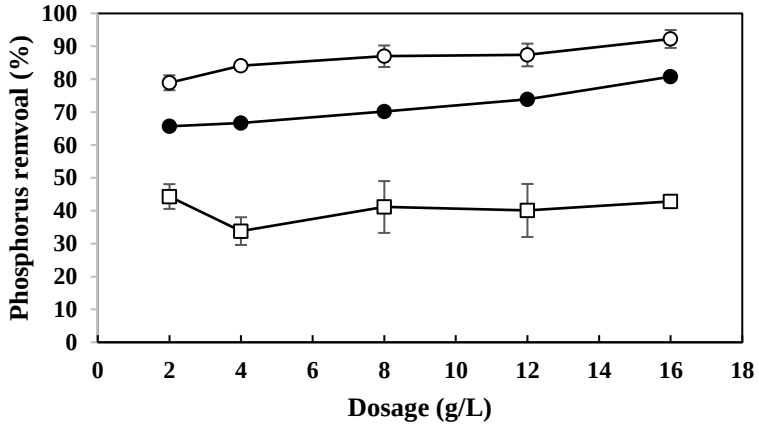

Figure 6. Effect of adsorbent dose on phosphate removal by (□) rice straw-derived biochar, (○) Fe(III) modified biochar and (●) Fe(III)+Fe(II) modified biochar (pH: 7; contact time: 24 h; PO_4-P: 2.5 mg/l).

4. Conclusions

Iron-modified biochar was prepared by pyrolysis of rice straw, followed by coating with iron oxides or hydroxides using two different treatments: direct precipitation of $FeCl_3.6H_2O$ and co-precipitation of $FeCl_3.6H_2O$ and $FeSO_4.7H_2O$. A pyrolysis temperature of 400°C led to the best combination of physicochemical properties related to contaminant sorption (i.e. specific surface area and stable organic matter yield index, SOMYI), and was used as the basis for loading iron onto the biochar surface. Some physicochemical properties (i.e. pH_{pzc}, elemental composition and surface functional groups) of both iron-modified biochars were similar, except Fe(III) loading led to a brownish color of biochar and contained more elemental iron than Fe(II)/Fe(III) combinations. Phosphate sorption assessment showed that the formation of iron hydroxides or oxides on the biochar surface significantly improved phosphate removal ability compared to unmodified biochar. Overall, this study showed that it is possible to turn an abundant agricultural residue, rice straw, effectively and cheaply into a value added product-iron-modified biochar, which efficiently removes phosphorus from water.

5. Acknowledgements

We thank the Department of Chemistry, Faculty of Science, KMITL for financial support for a student's Special Project of KD, NS and PP. Special thanks to John Morris, the author of "Keep it Simple" a guide to English Technical writing and a member of Research Clinic, KMITL Research and Innovation Services (KRIS) for removing unnecessary color and improving the readability of the paper.

References

[1] Kundu, S., Vassanda Coumar, M., Rajendiran, S., Kumar, A. and Subba Rao, A., 2015. Phosphates from detergents and eutrophication of surface water ecosystem in India. *Current Science*, 108(7), 1320-1325.

[2] Thawornchaisit, U., Kongtaweelert, S. and Kasibut, K., 2017. Preparation and evaluation of the alkaline-pretreated and Fe-modified pineapple peel for phosphate removal efficiency. *Proceedings of the International Research Conference on Sustainable Energy, Engineering, Materials and Environment*, Northumbria University, Newcastle Upon Tyne, England, July 26-28, 2017, 217-223.

[3] Duenas, J.F., Alonso, J.R., Rey, A.F. and Ferrer, A.S., 2003. Characterization of phosphorus forms in wastewater treatment plants. *Journal of Hazardous Materials*, 97, 193-205.

[4] Koottatep, T., Chapagain, S.K. and Polprasert, C., 2015. Situation and novel approach for sustainable phosphorus recovery: a case study of Thailand. *Global Environmental Research*, 19, 105-111.

[5] Karthikeyan, K.G., Tshabalala, M.A., Wang, D. and Kalbasi, M., 2004. Solution chemistry effects on orthophosphate adsorption by cationized solid wood residues. *Environmental Science & Technololgy*, 38(3), 904-911.

[6] European Commission, 2017. *Study on the review of the list of critical raw materials* [online] Available at: https://publications.europa.eu/en/publication-detail/-/publication/08fdab5f-9766-11e7-b92d-01aa75ed71a1/language-en. Accessed in April 2019.

[7] Ohtake, H., 2018. *Recovery, reuse of phosphorus from wastewater* [online] Available at: https://www.japantimes.co.jp/news/2018/09/14/national/recovery-reuse-phosphorus-wastewater/#.W_4No-gzbIW. Accessed in April 2019.

[8] Chen, B., Chen, Z. and Lv, S., 2011. A novel magnetic biochar efficiently sorbs organic pollutants and phosphate. *Bioresource Technology*, 102(2), 716-723.

[9] Mohan, D., Sarswat, A., Ok, Y.S. and Pittman, C.U. 2014. Organic and inorganic contaminants removal from water with biochar, a renewable, low cost and sustainable adsorbent – A critical review. *Bioresource Technology*, 160, 191-202.

[10] Ahmad, M., Rajapaksha, A.U., Lim, J.E., Zhang, M., Bolan, N., Mohan, D., Vithanage, M., Lee, S.S. and Ok, Y.S. 2014. Biochar as a sorbent for contaminant management in soil and water: A review. *Chemosphere*, 99, 19-33.

[11] Hameed, B.H. and El-Khaiary, M.I., 2008. Kinetics and equilibrium studies of malachite green adsorption on rice straw-derived char. *Journal of Hazardous Materials*, 153(1-2), 701-708.

[12] Qiu, Y., Zheng, Z., Zhou, Z. and Sheng, G.D., 2009. Effectiveness and mechanisms of dye adsorption on a straw-based biochar. *Bioresource Technology*, 100(21), 5348-5351.

[13] Li, H., Dong, X., da Silva, E.B., de Oliveira, L.M., Chen, Y. and Ma, L.Q., 2017. Mechanisms of metal sorption by biochars: Biochar characteristics and modifications. *Chemosphere*, 178, 466-478.

[14] Saadat, S., Raei, E. and Talebbeydokhti, N., 2018. Enhanced removal of phosphate from aqueous solutions using a modified sludge derived biochar: Comparative study of various modifying cations and RSM based optimization of pyrolysis parameters. *Journal of Environmental Management*, 225, 75-83.

[15] Beesley, L. and Marmiroli, M., 2011. The immobilisation and retention of soluble arsenic, cadmium and zinc by biochar. *Environmental Pollution*, 159(2), 474-480.

[16] Rajapaksha, A.U,. Chen, S.S., Tsang, D.C.W., Zhang, M., Vithanage, M., Mandal, S., Gao, B., Bolan, N.S. and Ok, Y.S., 2016. Engineered/designer biochar for contaminant removal/immobilization from soil and water: Potential and implication of biochar modification. *Chemosphere*, 148, 276-291.

[17] Vikrant, K., Kim, K.-H., Ok, Y.S., Tsang, D.C.W., Tsang, Y.F., Giri, B.S., Tsang, D.C.W., Tsang, Y.F., Giri, B.S. and Singh, R.S., 2018. Engineered/designer biochar for the removal of phosphate in water and wastewater. *Science of the Total Environment*, 616-617, 1242-60.

[18] International Rice Research Insititute, *Rice straw* [online] Available at: http://www.knowledgebank.irri.org/step-by-step-production/postharvest/rice-by-products/rice-straw. Accessed in May 2019.

[19] Food and Agriculture Organization of the United Nations, 2018. *Rice Market Monitor April 2018* [online] Available at: http://www.fao.org/economic/RMM. Accessed in May 2019.

[20] Department of Alternative Energy Department and Efficiency, Ministry of Energy. *Biomass Database Potential in Thailand* [online] Available at: http://biomass.dede.go.th/biomass_web/index.html. Accessed in May 2019.

[21] Yang, Q., Wang, X., Luo, W., Sun, J., Xu, Q., Chen, F., Zhao, J., Wang, S., Yao, F., Wang, D., Li, X. and Zeng, G., 2018. Effectiveness and mechanisms of phosphate adsorption on iron-modified biochars derived from waste activated sludge. *Bioresource Technology*, 247, 537-544.

[22] Land Development Department, 2004. *Manual for Analysis of Soils, Water, Fertilizers, Materials for Soil Improvement and Analysis for Certifying Commodity Standard* (in Thai). 2nd ed. Bangkok: Office of Science for Land Development.

[23] Hafshejani, L.D., Hooshmand, A., Naseri, A.A., Mohammadi, A.S., Abbasi, F. and Bhatnagar, A., 2016. Removal of nitrate from aqueous solution by modified sugarcane bagasse biochar. *Ecological Engineering*, 95, 101-111.

[24] Kaewprasit, C., Hequet, E.F., Abidi, N. and Gourlot, J.-P., 1998. Application of methylene blue adsorption to cotton fiber specific surface area measurement: Part I. Methodology. *Journal of Cotton Science*, 2(4), 164-173.

[25] American Public Health Association, American Water Works Association, Water Environment Federation. 2012. *Standard Methods for the Examination of Water and Wastewater*. 22nd ed. Washington, DC: APHA-AWWA-WEF.

[26] Jiang, J., Peng, Y., Yuan, M., Hong, Z., Wang, D. and Xu, R., 2015. Rice straw-derived biochar properties and functions as Cu(II) and cyromazine sorbents as influenced by pyrolysis temperature. *Pedosphere*, 25(5), 781-789.

[27] Wang, H., Chu, Y., Fang, C., Huang, F., Song, Y. and Xue, X., 2017. Sorption of tetracycline on biochar derived from rice straw under different temperatures. *PLoS One*, 12(8), e0182776.

[28] Masto, R.E., Kumar, S., Rout, T.K., Sarkar, P., George, J. and Ram, L.C., 2013. Biochar from water hyacinth (*Eichornia crassipes*) and its impact on soil biological activity. *Catena*, 111, 64-71.

[29] Ahmed, M.B., Zhou, J.L., Ngo, H.H., Guo, W. and Chen, M., 2016. Progress in the preparation and application of modified biochar for improved contaminant removal from water and wastewater. *Bioresource Technology*, 214, 836-851.

[30] Rafiq, M.K., Bachmann, R.T., Rafiq, M.T., Shang, Z., Joseph, S. and Long, R., 2016. Influence of pyrolysis temperature on physico-chemical properties of corn stover (*Zea mays* L.) biochar and feasibility for carbon capture and energy balance. *PLoS One*, 11(6), e0156894.

[31] Angın, D. and Şensöz, S., 2014. Effect of pyrolysis temperature on chemical and surface properties of biochar of Rapeseed (*Brassica napus* L.) *International Journal of Phytoremediation*, 16(7-8), 684-693.

[32] Angın, D., 2013. Effect of pyrolysis temperature and heating rate on biochar obtained from pyrolysis of safflower seed press cake. *Bioresource Technology*, 128, 593-597.

[33] González, J.F., Ramiro, A., González-García, C.M., Gañán, J., Encinar, J.M., Sabio, E. and Rubiales, J. 2005. Pyrolysis of almond shells. *Energy Applications of Fractions. Industrial & Engineering Chemistry Research*, 44, 3003-3012.

[34] Liao, T., Li, T., Su, X., Yu, X., Song, H., Zhu, Y. and Zhang, Y., 2018. La(OH)$_3$-modified magnetic pineapple biochar as novel adsorbents for efficient phosphate removal. *Bioresource Technology*, 263, 207-213.

[35] Komnitsas, K.A. and Zaharaki, D., 2016. Morphology of modified biochar and its potential for phenol removal from aqueous solutions. *Frontiers in Environmental Science*, 4, Article 26, 1-11. doi:10.3389/fenvs.2016.00026.

[36] Kulaksiz, E., Gözmen, B., Kayan, B. and Kalderis, D., 2017. Adsorption of malachite green on Fe-modified biochar: influencing factors and process optimization. *Desalination and Water Treatment*, 74, 383-394.

[37] Tang, Q., Shi, C., Shi, W., Huang, X., Ye, Y., Jiang, W., Kang, J., Liu, D.,Ren, Y. and Li, D., 2019. Preferable phosphate removal by nano-La(III) hydroxides modified mesoporous rice husk biochars: Role of the host pore structure and point of zero charge. *Science of the Total Environment*, 662, 511-520.

[38] Yin, Q., Zhang, B., Wang, R., and Zhao, Z., 2018. Phosphate and ammonium adsorption of sesame straw biochars produced at different pyrolysis temperatures. *Environmental Science & Pollution Research*, 25, 4320-4329.

[39] Yao, Y., Gao, B., Chen, J. and Yang, L., 2013. Engineered biochar reclaiming phosphate from aqueous solutions: Mechanisms and potential application as a slow- release fertilizer. *Environmental Science & Technology*, 47(15), 8700-8708.